Data-driven discovery of mechanisms underlying present and near-future precipitation changes and variability in Brazil

Márcia Talita A. Marques[1], Maria Luiza Kovalski[1], Gabriel M. P. Perez[1], Thomas C. M. Martin[1], Edson L. S. Y. Barbosa[1], Pedro Augusto S. M. Ribeiro[1], Roilan H. Valdes[2]

[1]MeteoIA, São Paulo, Brazil
[2]Engie Brazil, São Paulo, Brazil

Correspondence to: Gabriel M. P. Perez (gabriel@meteoia.com)

Abstract. Untangling the complex network of physical processes driving regional precipitation regimes in the present (1979-2014) and near-future climates (2020-2050) is fundamental to support a more robust scientific basis for decision making in the water-energy-food nexus. We propose a data-driven mechanistic approach to: (Goal 1) identify changes and variability of the regional precipitation mechanisms and (Goal 2) reduce the ensemble spread of future projections by weighting and filtering models that satisfactorily represent these drivers in present climate. Goal 1 is achieved by applying the Partial Least Squares (PLS) technique, a two-sided variant of principal component analysis (PCA), on a reanalysis dataset and 30 simulations of the future climate submitted to CMIP6 to discover the links between global sea-surface temperature (SST) and precipitation in Brazil. Goal 2 is achieved by selecting and weighting the future climate simulations from climate models that better represent the dominant modes discovered by the PLS in the present climate; with this subset of climate simulation, we produce precipitation change maps following IPCC's WG1 methodology. The main mechanistic link discovered by the technique is that the generalised warming of the oceans promotes a suppression of precipitation in Northeast and Southeast Brazil, possibly mediated by the intensification of the Hadley circulation. We show that this pattern of precipitation suppression is stronger in the near-future precipitation change maps produced using our methodology. This demonstrates that a reduction of epistemic uncertainty is achieved after we select models that skillfully represent these mechanisms in the present climate. Therefore, the approach is capable of supporting both a quantitative analysis of regional changes as well as the construction of storylines supported by mechanistic evidence.

1 Introduction

Information about near-future regional precipitation change is crucial for planning and managing critical infrastructure, such as hydropower plants, water reservoirs, and city planning. Unpreparedness for changes and variations in regional precipitation regimes may lead to disruption in the water-food-energy supply chains as well as avoidable deaths and damages by flooding and landslides. Although there is a degree of certainty about global precipitation changes (Shepherd et al., 2018),

such as the intensification of the hydrological cycle, a current major challenge in climate change science is informing planners and decision-makers about regional changes within the critical time-frame of the next three decades.

Within this time frame, the two main sources of uncertainty in regional precipitation changes are model uncertainty and internal variability (Hawkins and Sutton, 2011). Uncertainty due to the internal variability of the climate system is impossible to reduce and is aleatoric and related to the chaotic nature of the system (Shepherd, 2019). Model uncertainty, on the other hand, is epistemic in nature and stems from our limited knowledge of Earth's climate system and from the challenges in translating this system into computer models. Currently, there are 131 available models on the CMIP6 database, each representing Earth's climate with a range of parameterizations and numerical modelling strategies.

In this study, we seek for a reduction of the epistemic uncertainty of regional precipitation changes in Brazil through a data-driven process-based methodology of model selection and weighting. The method discovers the relationships between sea surface temperature and precipitation in Brazil and evaluates the capability of CMIP6 models to reproduce these precipitation mechanisms in the present climate. Later, the best models are selected and weighted to produce refined precipitation maps. Due to the process-based nature of the method, it is also possible to isolate mechanisms and draw storylines of plausible futures. The paper answers the following questions:

- What are the spatiotemporal links between global sea-surface temperature (SST) and regional precipitation change and variability in Brazil?¶
- Many patterns have been identified in the literature (Grimm et al., 2000; Coelho et al., 2002), but here we choose to use a supervised ML approach to systematically identify and quantify their importance
- Can we take advantage of these mechanisms to filter CMIP6 simulations and reduce the epistemic uncertainty of regional precip changes?
- ~~How precipitation will look like in the next 30 years in Brazil; as predicted by a filtered model ensemble, in which we can consider the mean, the trend or individual model runs as possible futures.~~ What are the predictions for precipitation in Brazil over the next 30 years based on a mechanistic filtering and weighting procedure?

2 Materials & Methods

2.1 Data-driven discovery of precipitation mechanisms

To discover the underlying mechanisms linking the SST spatiotemporal variability and regional precipitation in Brazil we employ a data-driven dimensionality reduction method known as Partial Least Squares (PLS) adapted to a ~~lat-lon~~ latitude-longitude grid; which has been recently shown to successfully identify circulation mechanisms leading to precipitation (Perez et al, 2022).

The PLS method identifies pairs of latent variable vectors ~~and~~ ξ and ω that maximises the information present in ~~XtY,~~X^tY. This means finding latents variables that represent the maximum covariance between X and Y, where X and Y represent two

arrays of SST and precipitation, respectively; rows of X and Y represent the monthly averaged temporal samples while the columns represent the spatial lat-lon grid points. The more familiar Principal Component Analysis (PCA) can be seen as a special case where X=Y. The initial set, or mode, of latent variables is determined through the following covariance Eq. (1):

~~$Cov(1,1) = max\|u\| = \|v\| = 1 Cov(Xu, Yv)$~~, $Cov(\xi_1, \omega_1) = max_{\|u\|=\|v\|=1} Cov(Xu, Yv)$,

(1)

where u and v are temporally invariant arrays of loadings; in contrast to PCA, PLS yields a pair of loading matrices per component rather than a single loading matrix; the first pair of loading matrices is the one in which the corresponding latent vectors ~~and~~ ξ and ω are ~~-~~ the most correlated. The following modes are found through repeating the process on the residuals of each preceding pair.

The interpretation of PLS results should always consider scores and loadings concurrently. A positive loading correlation, coupled with a positive trend in the scores, indicates an increase in signal strength over time. Conversely, when loadings exhibit the same signal but are associated with a negative trend in scores, this suggests a decrease in signal intensity. When evaluating the relationship between two loadings, we first observe how the loading patterns are linked through the score time series. This connection allows us to infer the response of the Y pattern from the X pattern. For instance, if the SST signal is negative at a particular location while the score is positive, this indicates a negative association with the corresponding precipitation loading pattern. A detailed explanation of the method can be found in Wegelin (2000).

2.2 Present and future climate datasets

The PLS method was applied to two kinds of climate datasets: firstly, to present climate data from AMIP experiments and reanalysis and, secondly, to the future climate simulations. In the AMIP experiments, atmospheric models are forced by prescribed sea surface temperatures. The subsections below describe the methodologies and data behind the present and future climate results.

2.2.1 Present climate (AMIP)

The first step was to establish a transfer function linking SST and precipitation month-to-month co-variability using the PLS technique, for the reanalysis and atmosphere-only experiments. The goal is to identify models that accurately represent the transfer function identified in the reanalysis in the present climate. To achieve this, we employ precipitation data derived from the ERA5 reanalysis (Hersbach and Dee, 2016), in addition to precipitation data from 29 AMIP models from the Coupled Model Intercomparison Project Phase 6 (CMIP6), as outlined in Table 1. Before the PLS technique was employed, the ERA5 precipitation data underwent systematic error correction using observations from the Global Precipitation Climatology Project (GPCP, Adler et al., 2018) as a reference through the quantile mapping method, which adjusts probability distributions by individually matching each quantile to the respective quantile of the reference dataset (Jakob et al., 2011). GPCP data has a shorter time period (from 1979) when compared to ERA5 data, which has been available since

1950. Since we aimed to investigate interannual/interdecadal variability and climate change, we chose the longer dataset. Each precipitation dataset was conservatively gridded to a regular 1°x1° lat-lon grid in a monthly temporal resolution between 1979 and 2014. SST data was obtained from the COBE dataset, produced by the Japan Meteorological Agency (Hiragana et al., 2014) , which has long temporal availability and is observations-based.

Table 1 - CMIP6 simulations, their native resolutions, vertical levels and source institutions

Model	Horizontal resolution	Vertical levels	Variant label	Institution
ACCESS-CM2	1.875° × 1.25°	85	r1i1p1f1	CSIRO
ACCESS-ESM1-5	1.875 ° x 1.25°	38	r1i1p1f1	CSIRO
BCC-CSM2-MR	2.81° x 2.81°	46	r1i1p1f1	BCC
CAMS-CSM1-0	1° x 1°	31	r1i1p1f1	CAMS
CanESM5	2.81° x 2.81°	49	r1i1p1f1	CCCma
CESM2-WACCM	0.9° x 1.25°	70	r1i1p1f1	NCAR
CIESM	1° x 1°	30	r1i1p1f1	THU
CMCC-CM2-SR5	1° x 1°	30	r1i1p1f1	CMCC
CNRM-CM6-1	1.4° x 1.4°	91	r1i1p1f2	CNRM-CERFACS
CNRM-CM6-1-HR	1.4° x 1.4°	91	r1i1p1f2	CNRM-CERFACS
CNRM-ESM2-1	1.4° x 1.4°	91	r1i1p1f2	CNRM-CERFACS
EC-Earth3-CC	0.7° x 0.7°	91	r1i1p1f1	EC-Earth-Consortium
EC-Earth3-Veg	0.7° x 0.7°	91	r1i1p1f1	EC-Earth-Consortium
EC-Earth3-Veg-LR	1.1° x 1.1°	62	r1i1p1f1	EC-Earth-Consortium
FGOALS-f3-L	1° x 1°	32	r1i1p1f1	IAP/CAS
FGOALS-g3	2° x 2°	26	r1i1p1f1	IAP/CAS
GFDL-CM4	1° x 1°	33	r1i1p1f1	NOAA-GFDL
GFDL-ESM4	1° x 1°	49	r1i1p1f1	NOAA-GFDL
IITM-ESM	2° x 2°	64	r1i1p1f1	CCCR-IITM
INM-CM4-8	2° x 1.5°	21	r1i1p1f1	INM
INM-CM5-0	2° x 1.5°	73	r1i1p1f1	INM
IPSL-CM6A-LR	2.5° x 1.3°	79	r1i1p1f1	IPSL
KACE-1-0-G	1.9° x 1.3°	85	r1i1p1f1	NIMS-KMA
MIROC6	1.4° x 1.4°	81	r1i1p1f1	MIROC
MPI-ESM1-2-HR	0.93° x 0.93°	95	r1i1p1f1	MPI-M
MPI-ESM1-2-LR	1.9° x 1.9°	47	r1i1p1f1	MPI-M

Model	Horizontal resolution	Vertical levels	Variant label	Institution
ACCESS-CM2	1.875° × 1.25°	85	r1i1p1f1	CSIRO
MRI-ESM2-0	1.125° x 1.125°	80	r1i1p1f1	MRI
NESM3	1.9° x 1.9°	47	r1i1p1f1	NUIST
NorESM2-LM	2° x 2°	32	r1i1p1f1	NCC
TaiESM1	1.25° x 0.9°	30	r1i1p1f1	AS-RCEC

The models listed above, through their computational representations of the atmosphere, choices of parameterisation, vertical levels etc, provide unique numerical representations of the physical climate system. Each of these representations have a distinct level of skill in simulating the mechanisms of precipitation variability and changes in Brazil. Therefore, we rank and select the models with higher performance to represent the SST-precipitation transfer function revealed by the PLS analysis. This ranking is based on the Normalised Root Mean Square Error (NRMSE), which is obtained by comparing the PLS scores and loadings ~~between each model and those derived from the ERA5 reanalysis. Models that exhibit NRMSE < 0.6 in at least two out of the first four PLS components, are singled out as more reliably representing mechanisms that cause the precipitation in Brazil while the rest is discarded for the remaining analysis.~~, for each x and y information, between every single model and those derived from the ERA5 reanalysis. In other words, the X score of model A had its correlation calculated with the X score of ERA5, and so on. That means, the scores and loadings were separately calculated and after that, used a normalisation. The models that exhibit NRMSE values below 0.6 in at least two out of the first four PLS components were selected. This value is chosen after a visual analysis of all the PLS components among the models. These selected models are singled out as more reliably representing mechanisms that cause the precipitation in Brazil while the rest is discarded for the remaining analysis.

After the model ranking and selection step, we provide a set of weights that will be later used for model averaging. This set of weights is found by multiplying the inverse of the NRMSE by the importance of each PLS component; this is done so that models that perform well in representing more relevant mechanisms are favoured during the model pooling step. The importance of each PLS component is quantified by the coefficient of determination (r^2) of the reconstructed precipitation using only that component and the original ERA5 precipitation.

2.2.2 Future climate

We employ the same PLS methodology on future climate simulations under the SSP2-2.45 scenario between 2020 and 2050; in this near-future temporal range, we do not expect the choice of scenario to influence the results because scenario uncertainty in regional precipitation changes only becomes relevant in later decades (Hawkins and Sutton, 2011).

Finally, the effectiveness of this methodology in reducing the uncertainty of near-future precipitation changes in the CMIP6 ensemble is assessed by comparing the uncertainty of all CMIP6 models listed in Table 1 with the uncertainty of the subset of models selected by our methodology. ~~The uncertainty of the climate change signal was computed for each grid cell by determining the ratio (in %) between the ensemble mean climatologies of the SSP2-4.5 scenario for the years 2020-2050 and the historical period of 1979-2014.~~The climate change signal was computed for each grid cell by calculating the ratio (in %) between the anomaly of the ensemble mean climatologies of the SSP2-4.5 scenario for the years 2020-2050 and the historical period of 1979-2014, divided by the historical. To assess the robustness of the models, we apply the procedure adopted by the Intergovernmental Panel on Climate Change (IPCC), as outlined in its Sixth Assessment Report, made available through the Interactive Atlas developed by Working Group I (WGI). This approach determines the robustness of climate change signals based on a strong model consensus, highlighting where at least 80% of the models agree on the sign of the predicted changes.

3 Results and discussion

In this section, we present the results of the analysis for the present and future climates, discussing the underlying precipitation mechanisms in reanalysis and model data. We also discuss the reduction of epistemic uncertainty of regional precipitation changes obtained through the selection of models that skillfully represent precipitation mechanisms in the present climate. In all ~~results~~PLS analysis, the Legal Amazon area was cropped off; this is because precipitation in the Amazon region presents significantly higher variability in magnitude, dominating the results and washing out patterns in other areas that are also socioeconomically relevant.

3.1 Precipitation mechanisms in the present climate (1979-2014)

In the present climate, the first PLS loadings matrix of the SST reveals a prominent positive pattern in the central Pacific Ocean that aligns with the region dominated by the El Niño/Southern Oscillation (ENSO) phenomenon (Fig. 1a). This ENSO-like pattern with high statistical significance (unhatched area) extends from the west coast of South America to the Maritime Continent in the equatorial region, surrounded by a pattern of opposite signal. There is a negative trend in Fig. 1c scores, indicating a change of sign in the patterns of Fig. 1a. This suggests that in the first half of the timeseries, El Niño conditions were dominant, while in the second half of the time series, La Niña conditions were. The associated PLS loadings matrix for precipitation shows a significant positive correlation in South Brazil and a negative correlation in Northeast Brazil (Fig. 1b). The time series of the associated scores do not show a strong linear trend, reinforcing that this PLS mode is more associated with a natural variability mechanism like ENSO than to climate change (Fig. 1d).

The global warming trend can explain the mostly positive SST loadings matrix and the increasingly positive scores time series of the second PLS component (Fig. 2a,c). This warming oceanic pattern is linked to a precipitation reduction in most of Southeast and Northeast Brazil (Fig. 2b,d). A possible explanation for this precipitation suppression is the expansion of

the Hadley cell under climate change (Lu et al., 2007; Grise & Davis, 2020) and, consequently, the restriction of the equatorward motion of extratropical cyclones and their fronts, which are important precipitation mechanisms in Southeast Brazil (Perez et al., 2021). Perez et al. (2022) has shown that a temporary intensification of the Hadley circulation during positive NAO events leads to precipitation suppression in Southeast Brazil.

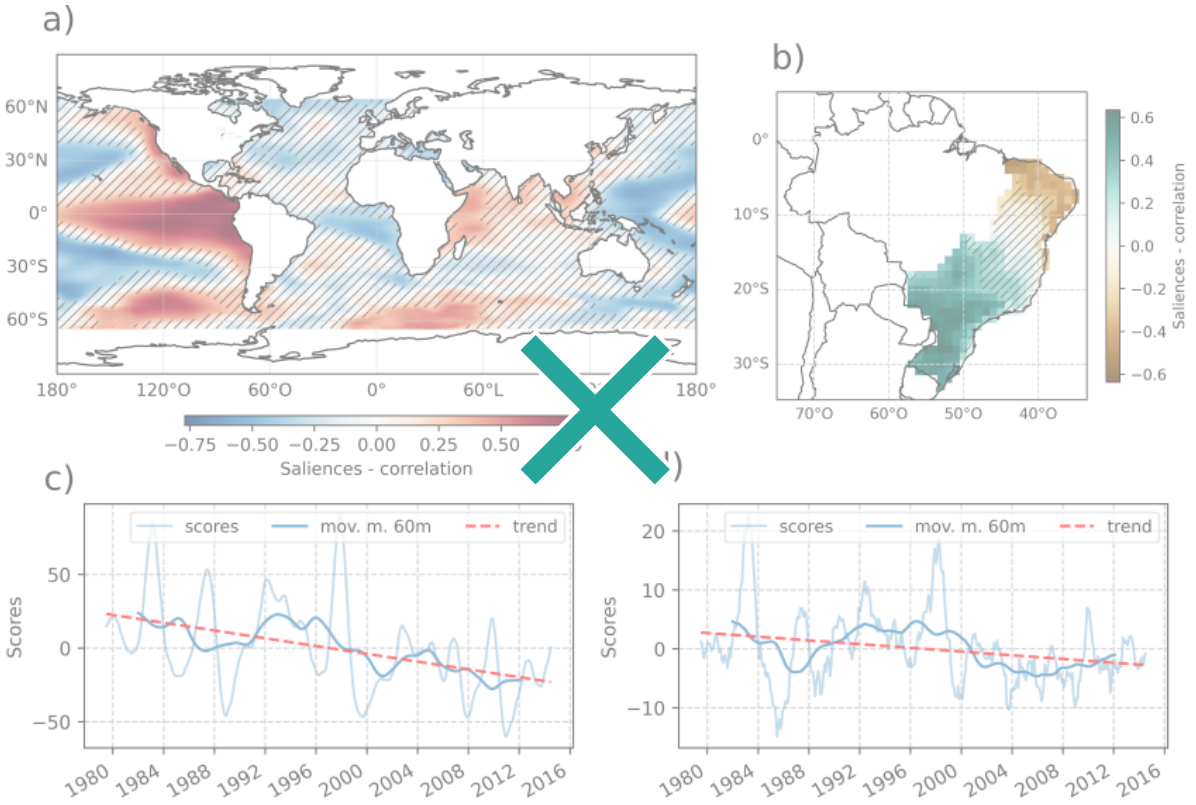
a)
60°N
30°N
0°
30°S
60°S
180°
120°O
60°O
0°
60°L
180°
−0.75 −0.50 −0.25 0.00 0.25 0.50
Saliences - correlation
b)
0°
10°S
20°S
30°S
70°O
60°O
50°O
40°O
0.6
0.4
0.2
0.0
−0.2
−0.4
−0.6
Saliences - correlation
c)
scores
mov. m. 60m
trend
Scores
50
0
−50
1980
1984
1988
1992
1996
2000
2004
2008
2012
2016
scores
mov. m. 60m
trend
Scores
20
10
0
−10
1980
1984
1988
1992
1996
2000
2004
2008
2012
2016

156

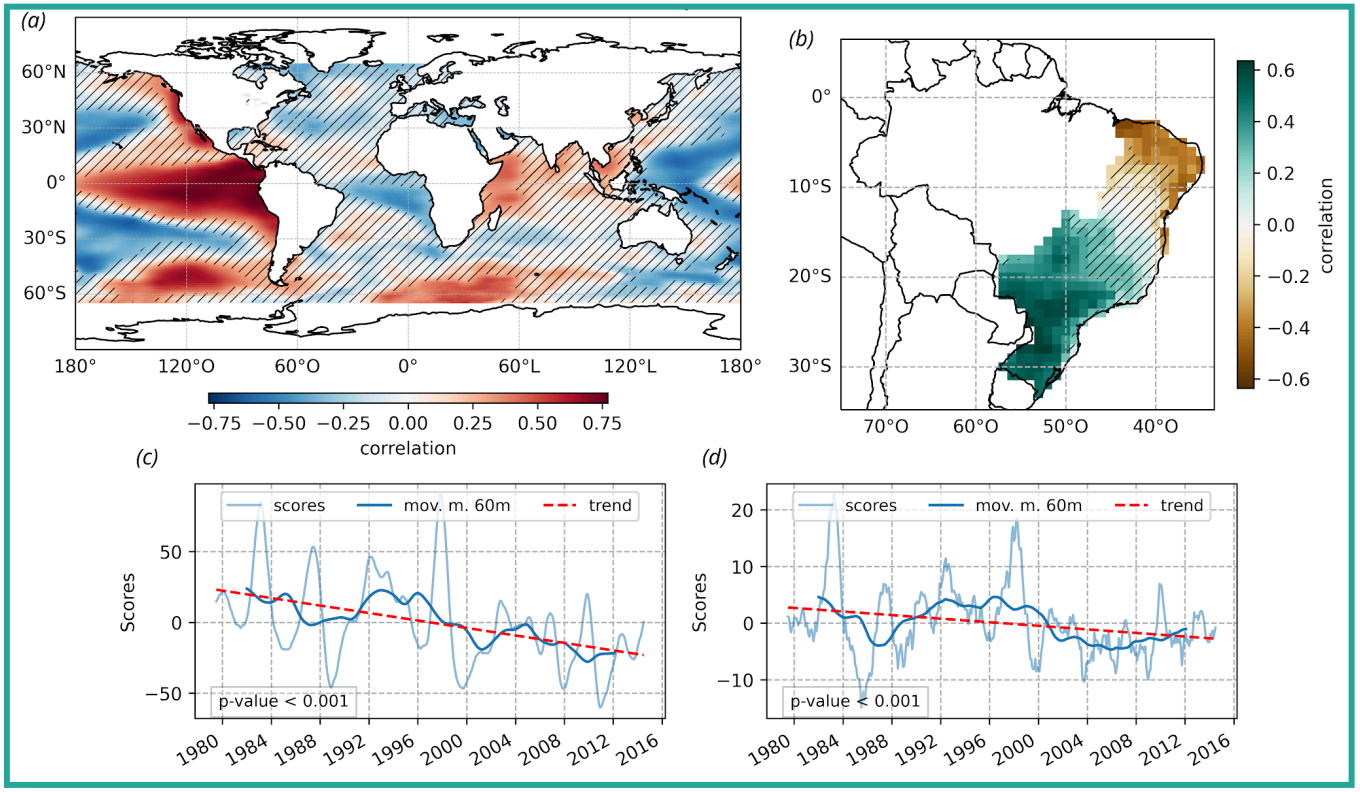

Figure 1: First component of the PLS methodology applied using monthly precipitation data from ERA5 and SST data from COBE between 1979 and 20154. The spatial maps represent the loadings matrices and the time series represent the scores. The hatchings represent areas where the statistical confidence on the sign of the anomaly is lower than 95%. The p-values indicate the statistical significance of the results.

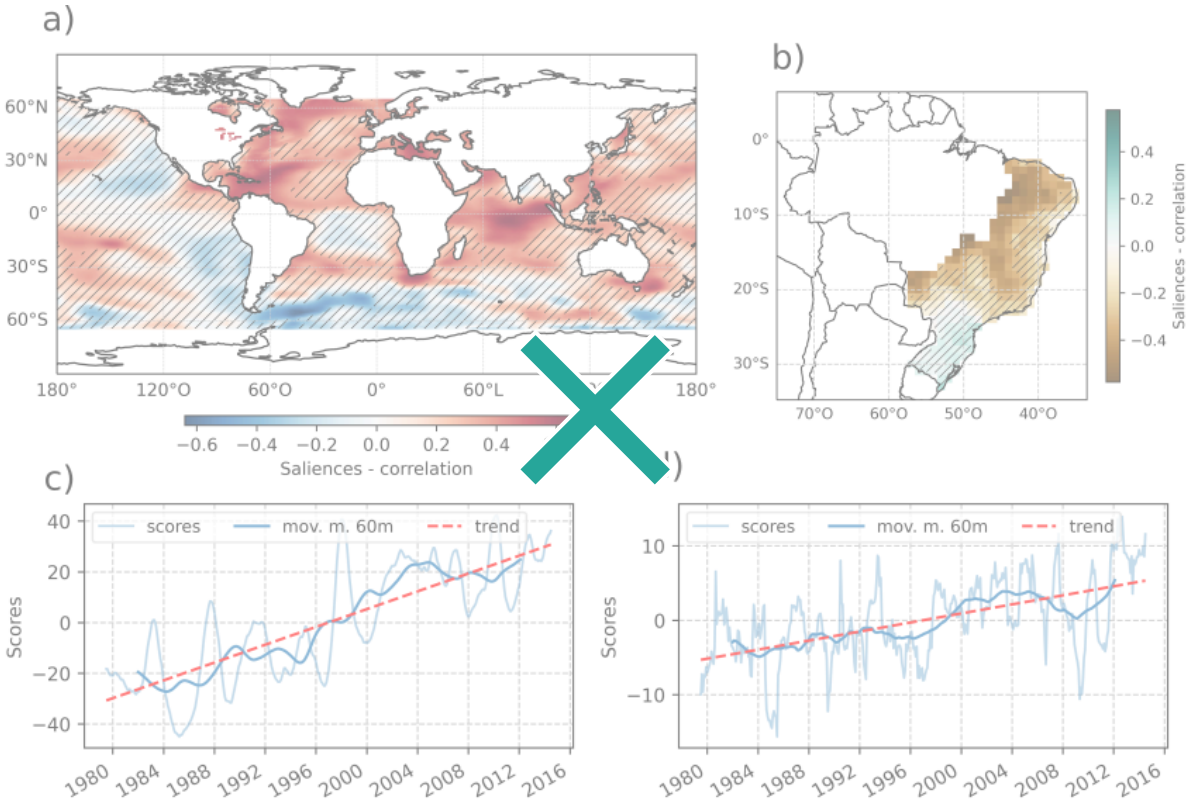
a)
60°N
30°N
0°
30°S
60°S
180°
120°O
60°O
0°
60°L
180°
−0.6 −0.4 −0.2 0.0 0.2 0.4
Saliences - correlation
b)
0°
10°S
20°S
30°S
70°O
60°O
50°O
40°O
0.4
0.2
0.0
−0.2
−0.4
Saliences - correlation
c)
scores
mov. m. 60m
trend
Scores
40
20
0
−20
−40
1980
1984
1988
1992
1996
2000
2004
2008
2012
2016
d)
scores
mov. m. 60m
trend
Scores
10
0
−10
1980
1984
1988
1992
1996
2000
2004
2008
2012
2016

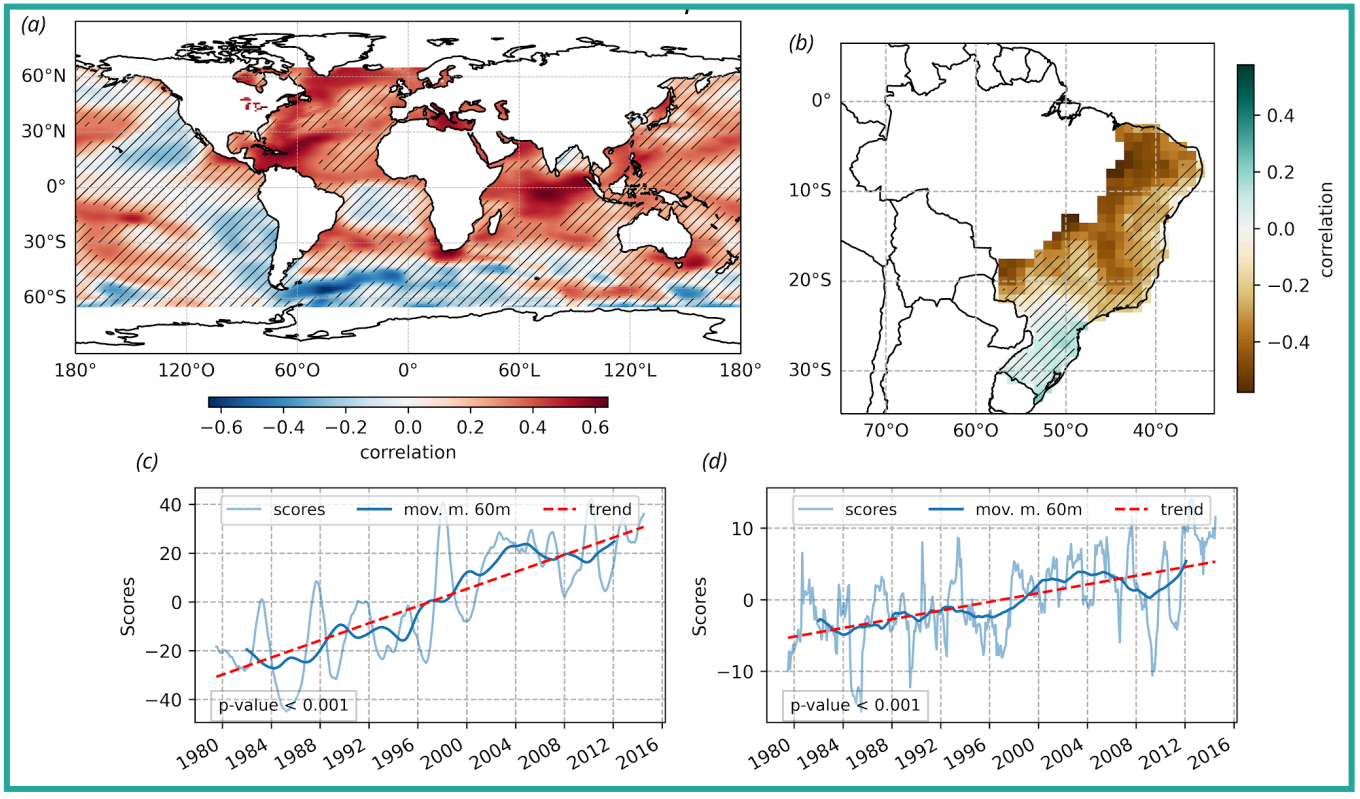

Figure 2 - Second component of the PLS methodology applied using monthly precipitation data from ERA5 and SST data from COBE between 1979 and 2014. The spatial maps represent the loadings matrices and the time series represent the scores. The hatchings represent areas where the statistical confidence on the sign of the anomaly is lower than 95%. The p-values indicate the statistical significance of the results.

For the third and fourth components (Annex), we observe more divergence in the results. Despite this, we consider these components in our evaluation due to their assigned weights and the potential for providing additional representation of driving mechanisms beyond the first and second components. Moreover, these third and fourth components might reveal important patterns that affect precipitation in Brazil, especially the Atlantic SST variability (Hastenrath and Greischar, 1993; Yoon and Zeng, 2010; Perez et al, 2022).

Through the analysis of the PLS components in the present climate datasets, we are able to select and rank the models based on their performance to reproduce these components. The model selection is based on a threshold of NRMSE< 0.6, and the individual model weights are based on the inverse of the average NRMSE among the PLS components scaled by the importance of each component, as described in the Methodology section. The table ~~below~~2 lists the selected models and their respective weights along with the components these models skillfully represent, later employed to construct the weighted ensemble mean in the future climate section. These models selected through our approach are those that showed better performance in the task of simulating the impacts of precipitation in Brazil. This way, for example, the high weight of GFDL-ESM4, indicates that this model performs well in representing the overall components more accurately when compared to other models. While it is true that component 1 relates to the ENSO dynamics, the overall evaluation takes into

components that represent other important forcings of the Brazilian precipitation regime. For instance, the Atlantic SST variability drives the Brazilian precipitation variability in the Amazon (Yoon and Zeng, 2010), Northeast Brazil (Hastenrath and Greischar, 1992) and subtropical regions (Perez et al., 2022). Furthermore, by including multiple components in the analysis, we acknowledge that climate dynamics are multifaceted, and a comprehensive evaluation should account for more than just the primary modes of variability like ENSO. This approach rests on the importance of a holistic evaluation of model performance across various components, rather than focusing solely on the primary modes.

Table 2 - List of selected models and their weights represented as a percentage of their contribution to the ensemble mean.

Model	Components	Weight (%)
CAMS-CSM1-0	1, 2, 4	7.76
CNRM-ESM2-1	1, 3, 4	7.73
GFDL-ESM4	2, 4	7.59
BCC-CSM2-MR	1, 2, 4	7.37
EC-Earth3-CC	1, 2	7.11
EC-Earth3-Veg-LR	1, 2	7.08
EC-Earth3-Veg	2, 4	6.83
IPSL-CM6A-LR	2, 3, 4	6.69
KACE-1-0-G	1, 2	6.61
CNRM-CM6-1-HR	2, 3, 4	6.56
MPI-ESM1-2-HR	1, 4	6.28
CMCC-CM2-SR5	1, 2	6.19
FGOALS-f3-L	2, 3	6.18
MIROC6	1, 4	5.94
CESM2-WACCM	1, 4	4.08

3.2 Precipitation mechanisms in the future climate (2020-2050)

The oceanic mechanisms driving precipitation in Brazil in the future climate (2020-2050) are discovered by applying the PLS methodology in CMIP6 future climate simulations (Fig. 3 and 4). Figure 3 shows the first PLS component and Figure 4 the second PLS component; for each component, only models that performed well (NRMSE < 0.6) in the present climate are considered. The spatial maps show the average loadings matrices of the model ensemble, where each model is weighed by its skill in the present climate (Table 2); the hatched areas represent regions where at least 80% of the models disagree on the sign of the loadings matrix.

The first component shows a strong Niño-like pattern in the Central Pacific, similarly to what is found in the present climate (Fig. 3a). However, unlike the present climate analysis, this Niño-like component shows a strong linear trend in the time series of scores (Fig. 3c), suggesting that the climate models are mixing the natural variability of the ENSO phenomenon and anthropogenic global warming; this warming trend can also be seen in the increasingly positive patterns in the tropical Atlantic and Indian oceans. The impact of this warming trend in the Brazilian regional precipitation is a wetting pattern in South Brazil and a drying pattern in Northeast Brazil, interfaced by a large region of uncertainty (Fig. 3b).

The second component illustrates a generalised warming trend in most regions of model agreement (Fig. 4a,c). This component impacts precipitation in Brazil through a drying trend in the southernmost border of the country and a wetting trend in the southeastern area. Some coastal areas in Northeast Brazil are significantly affected by a drying trend (Fig. 4b,d). Although the linear trend was observed in most models (Fig. 3c,d and Fig. 4c,d), it becomes clearer and more robust in the model subset; this reflects how sifting models in a mechanistic approach helps reduce the epistemic uncertainties.

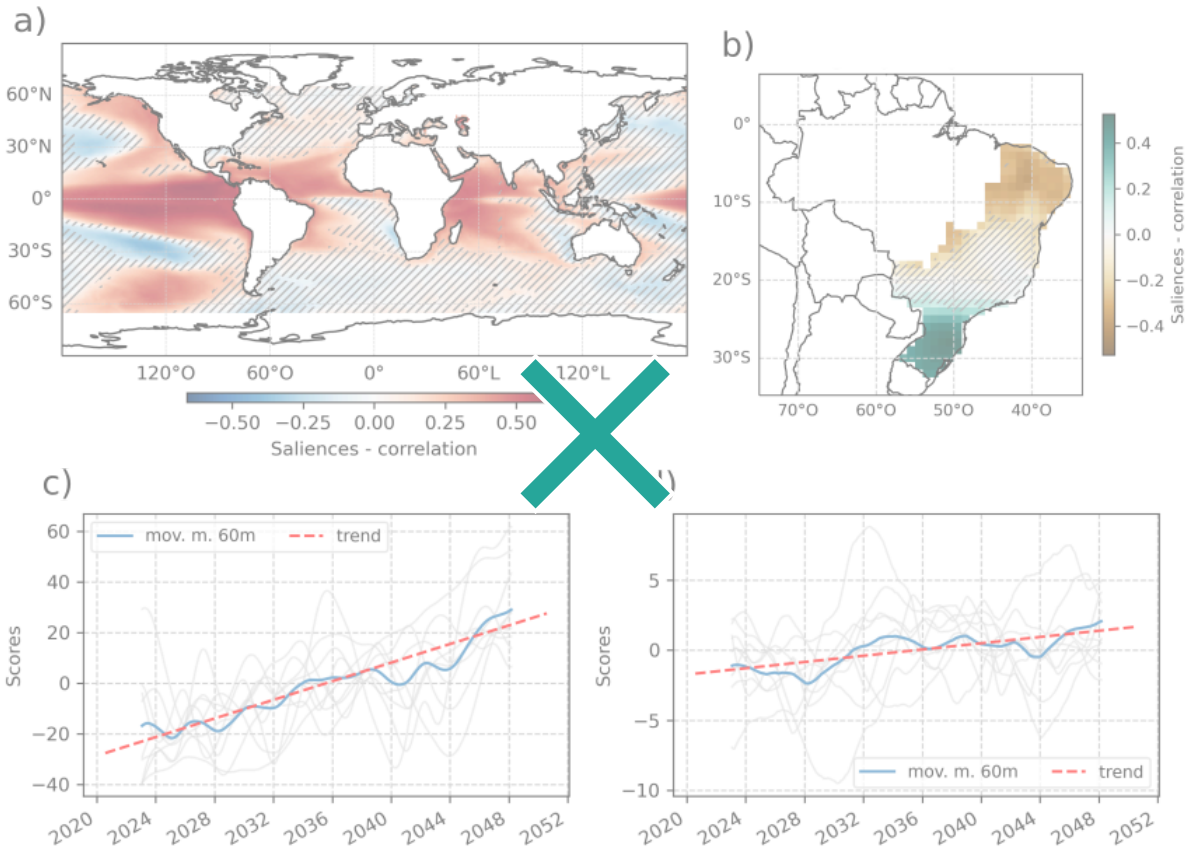
a)
60°N
30°N
0°
30°S
60°S
120°O
60°O
0°
60°L
120°L
−0.50 −0.25 0.00 0.25 0.50
Saliences - correlation
b)
0°
10°S
20°S
30°S
70°O
60°O
50°O
40°O
0.4
0.2
0.0
−0.2
−0.4
Saliences - correlation
c)
mov. m. 60m
trend
Scores
60
40
20
0
−20
−40
2020
2024
2028
2032
2036
2040
2044
2048
2052
mov. m. 60m
trend
Scores
5
0
−5
−10

209

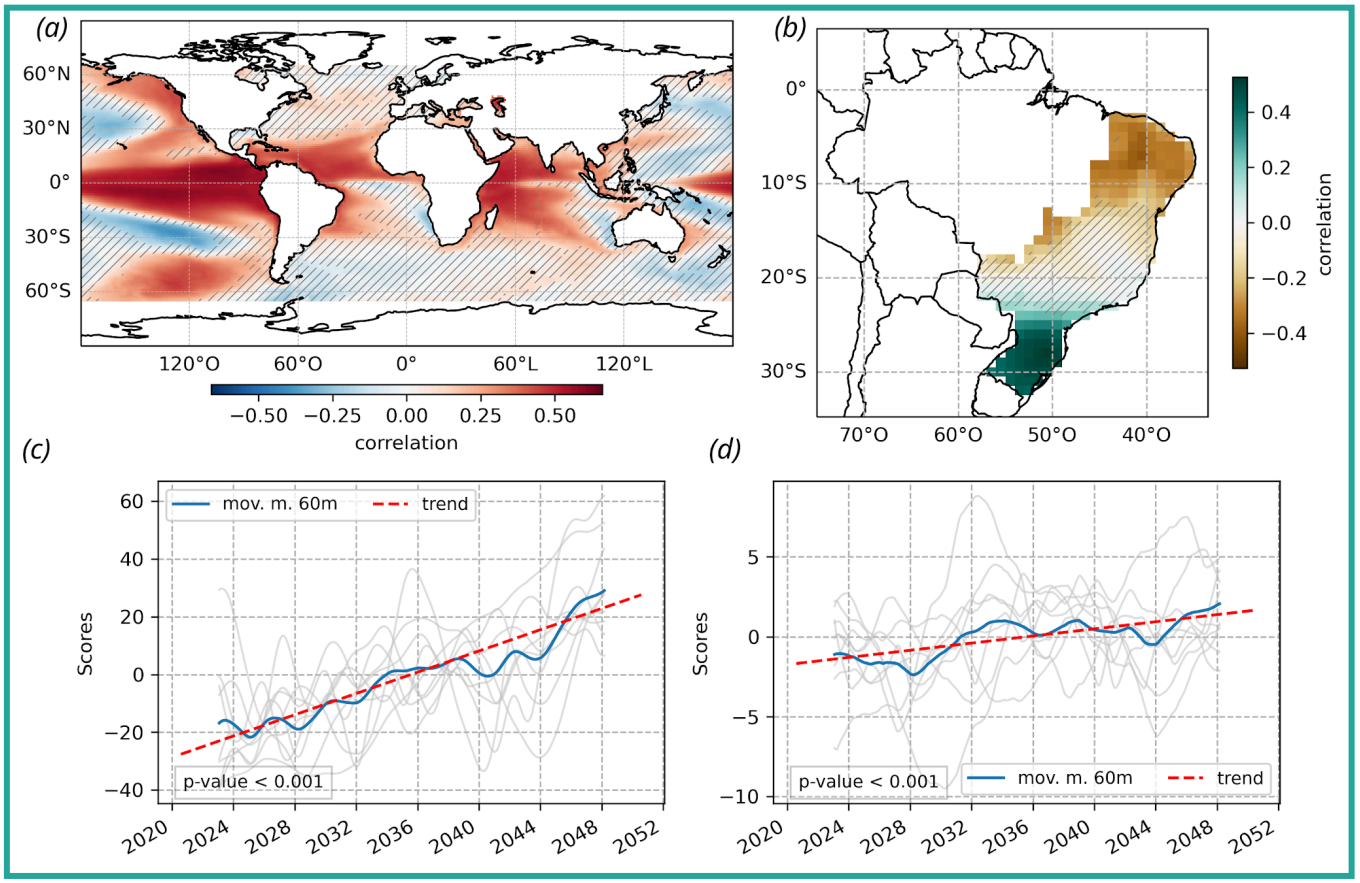

Figure 3 - First component of the PLS methodology applied using monthly precipitation data from CMIP6 models under the SSP2-4.5 scenario, listed in Table 2, between 2020 and 2050. The spatial maps represent the loadings matrices and the time series represent the scores. The regions with hatching indicate areas of uncertainty with < 80% agreement in the sign change among the models. The p-values indicate the statistical significance of the results.

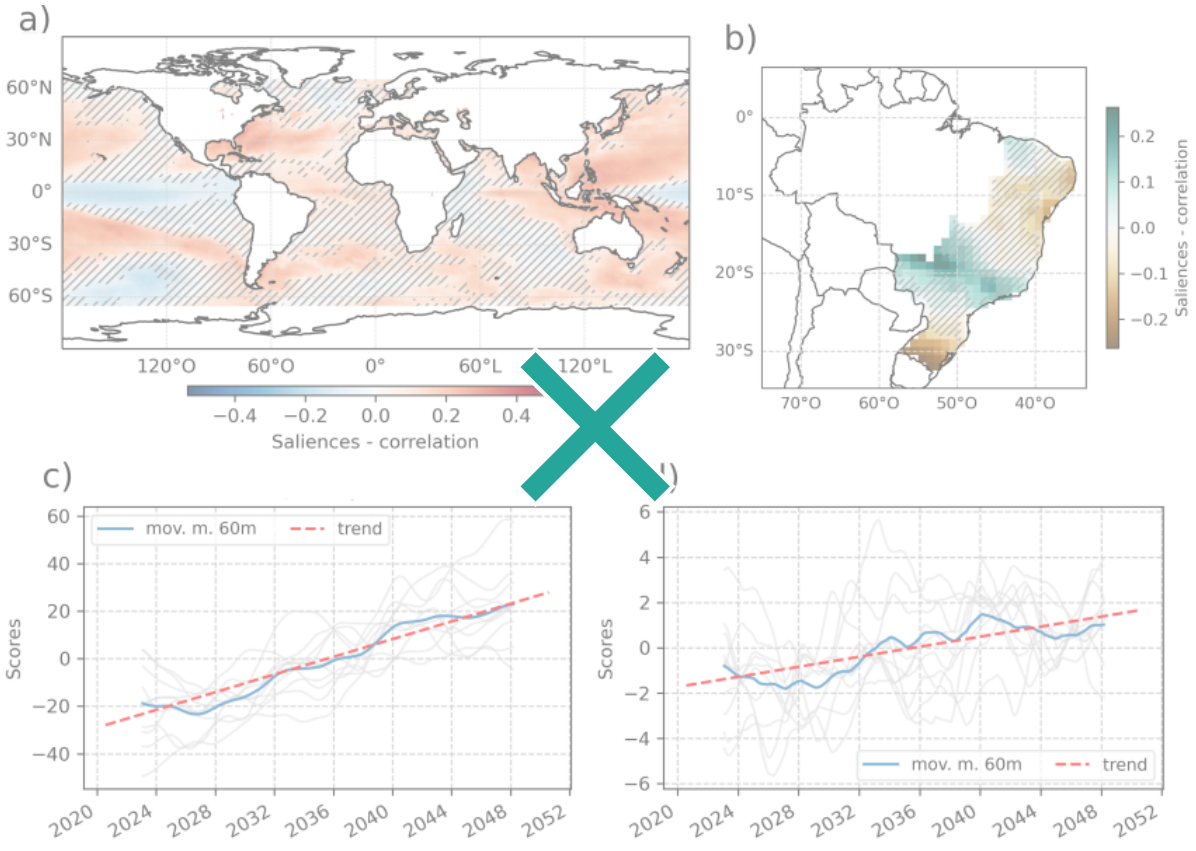
a)
60°N
30°N
0°
30°S
60°S
120°O
60°O
0°
60°L
120°L
−0.4
−0.2
0.0
0.2
0.4
Saliences - correlation
b)
0°
10°S
20°S
30°S
70°O
60°O
50°O
40°O
0.2
0.1
0.0
−0.1
−0.2
Saliences - correlation
c)
mov. m. 60m
trend
Scores
60
40
20
0
−20
−40
2020
2024
2028
2032
2036
2040
2044
2048
2052
d)
mov. m. 60m
trend
Scores
6
4
2
0
−2
−4
−6
2020
2024
2028
2032
2036
2040
2044
2048
2052

215

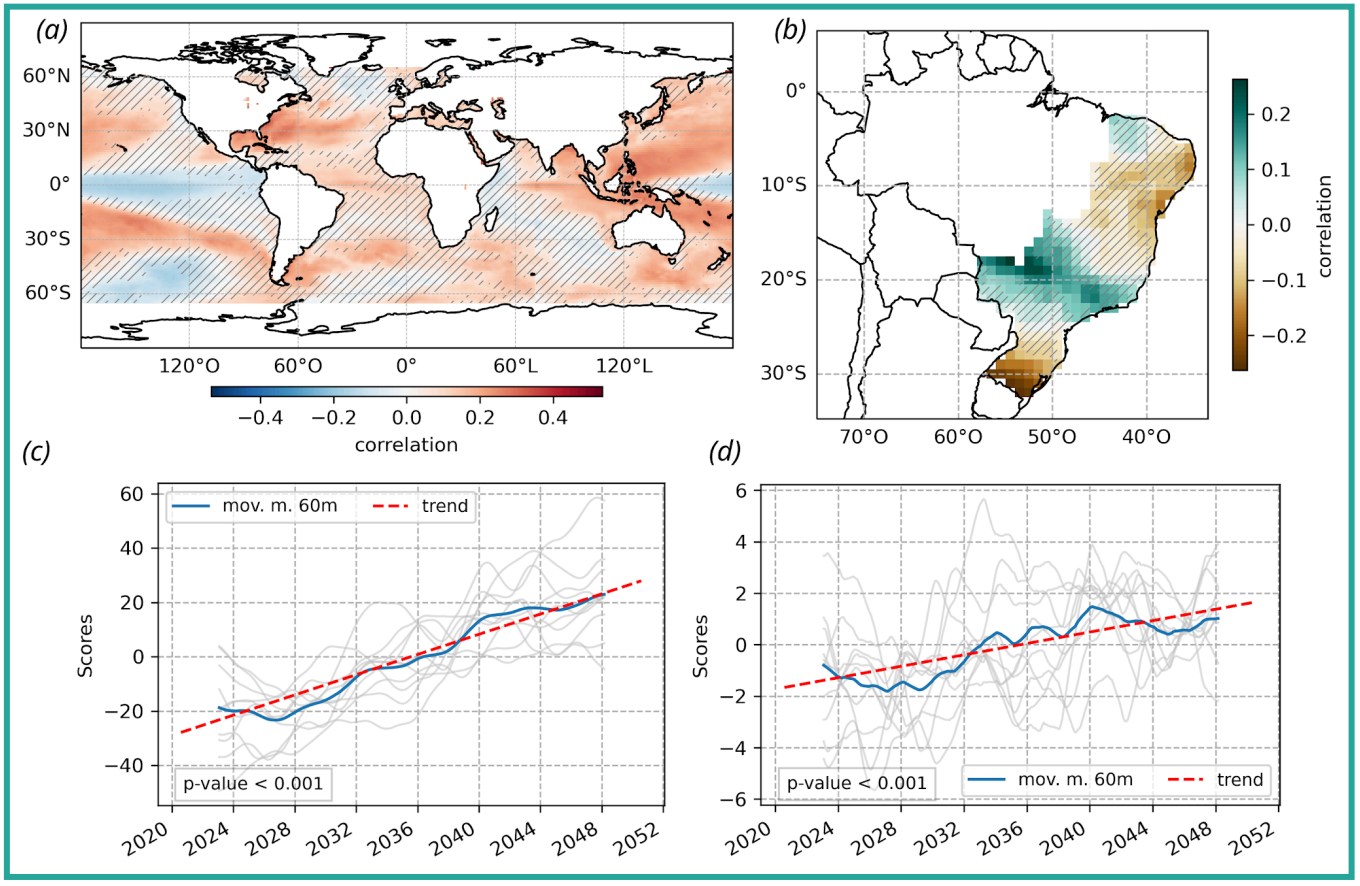

Figure 4 - Second component of the PLS methodology applied using monthly precipitation data from CMIP6 models under the SSP2-4.5 scenario, listed in Table 2, between 2020 and 2050. The spatial maps represent the loadings matrices and the time series represent the scores. The regions with hatching indicate areas of uncertainty with < 80% agreement in the sign change among the models. The p-values indicate the statistical significance of the results.

3.3 Future climate precipitation changes and uncertainty reduction

While the analysis of individual PLS components may support storyline approaches and mechanistic understanding, a quantitative precipitation change map is often required by decision-making bodies. With that in mind, we provide an uncertainty map based on the methodology employed by the IPCC in its 6th Assessment Report (Fig. 5). Here, we focus on the percentage of projected changes in 2020-2050 relative to 1979-2014. The hatching highlights regions where there is a significant lack of consensus, with at least 80% of the models analysed showing non-concordance, similar to the PLS uncertainty maps shown in the previous section.

Figure 5a shows the ensemble mean of the future precipitation changes using all CMIP6 models, listed in Table 1, while Fig. 5b uses the mean of the subset of models in Table 2 weighted by their skill in simulating precipitation mechanisms in the present climate (Fig. 5b). Firstly, we notice that the reduction of epistemic uncertainty by the proposed methodology is revealed by stronger anomalies and fewer hatched areas. Particularly, the South Atlantic Subtropical High (SASH) shows

stronger negative anomalies, suggesting a trend towards drier conditions in the region via an intensification of the Hadley cell descending branch. Moreover, the positive changes in South Brazil have increased after the application of the methodology; this enhanced dipole between the SASH and South Brazil is consistent with the mechanism of restriction of cold fronts revealed by the PLS in the present climate and discussed in Sect. 3a. In other words, selecting and weighting models that reproduce important precipitation mechanisms in the present climate has increased the clarity of what may happen in the region in the near-future climate.

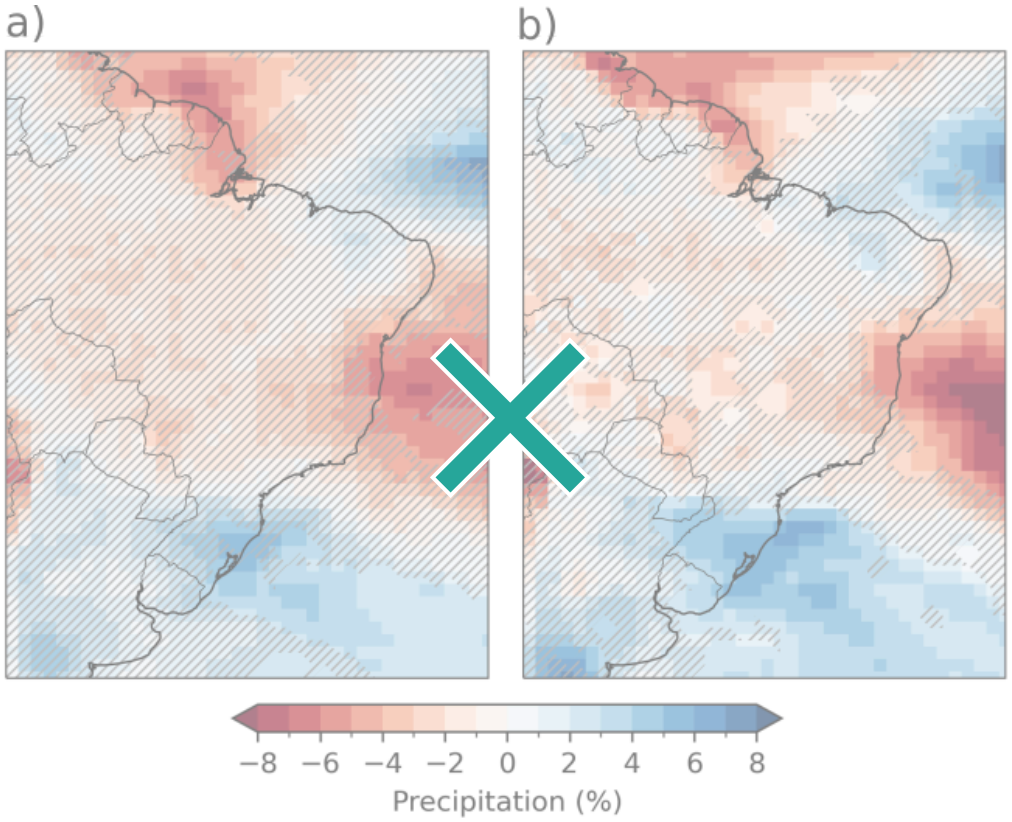

238

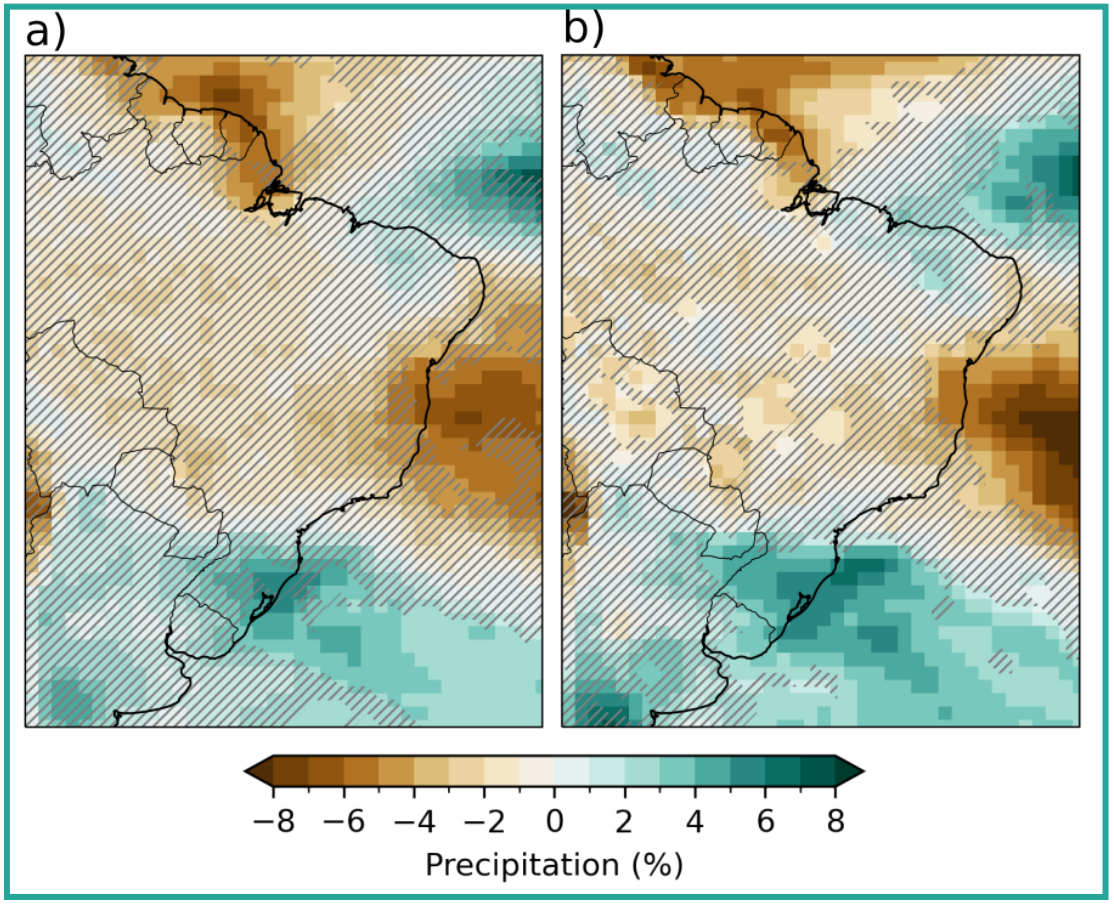

Figure 5 - Percentual precipitation changes in 2020-2050 relative to 1979-2014 based on all assessed models, as listed in Table 1, (a) and the percentual changes based on the selected models listed in Table 2 (b) from CMIP6 under the SSP2-4.5 scenario. The regions with hatching indicate areas of uncertainty with < 80% agreement in the sign change among the models.

Figure 6 shows the future precipitation changes broken down by season based on all models listed in Table 1 and only using the models selected by the methodology (Table 2). A noticeable reduction of uncertainty across all seasons is evident when comparing the hatched areas using all models versus only using the selected models, underscoring the success of our process-based model selection methodology in enhancing our confidence in regional climate projections. The period from December to May corresponds to the rainy season, characterised by a prevalence of uncertainties; this is in agreement with Bazzanela et al. (2023) and Firpo et al. (2022), that also indicate that CMIP6 models perform better in the dry season than in the wet season.

From June to November the Central and Northeast regions exhibit a clear drying pattern. In JJA, in particular, precipitation in most of Brazil is largely driven by cold fronts, which, as previously discussed, can be restrained in higher latitudes if the SASH is intensified. In SON, we expect an intensified SASH to also contribute to a later onset of the rainy season. This drying pattern in JJA and SON is intensified in the subset of selected models. This is unsurprising, since the SASH

subsidence associated with an intensification of the Hadley circulation is one of the mechanisms discovered by the PLS analysis in the present climate and used to select the best performing models.

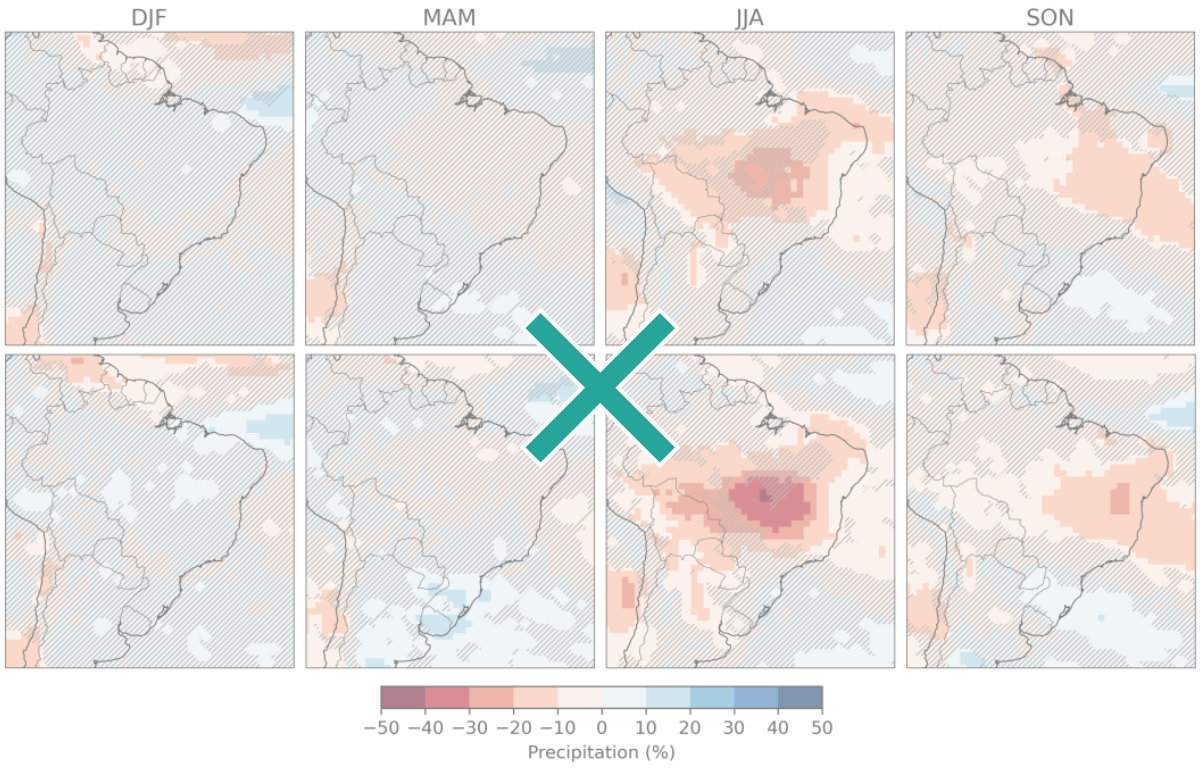

256

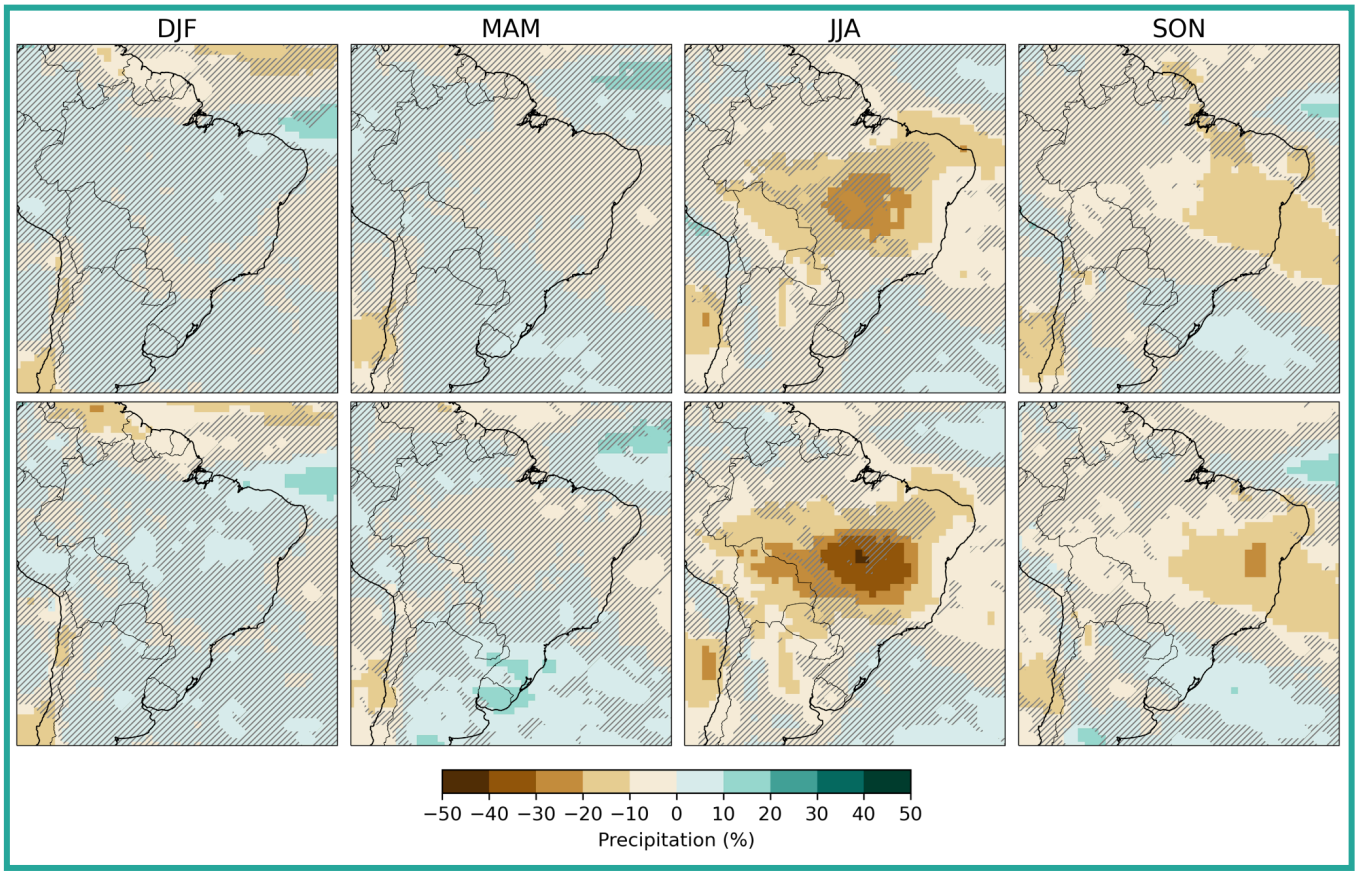

Figure 6 - Seasonal percentual precipitation changes in 2020-2050 relative to 1979-2014 based on all assessed models, as listed in Table 1, (up) and the percentual changes based on the selected models listed in Table 2 (down) from CMIP6 under the SSP2-4.5 scenario. The regions with hatching indicate areas of uncertainty with < 80% agreement in the sign change among the models.

4 Summary and Conclusions

This study aims to reduce the epistemic uncertainty of regional precipitation changes in Brazil through a data-driven process-based methodology of model selection and weighting. To achieve this, we first employ the methodology to discover the main precipitation drivers in the present climate (1979-2014) in a reanalysis dataset (Sect. 3a), revealing that the El Niño and the generalised warming of the oceans are linked to significant precipitation impacts in Brazil (Fig. 1 and 2). A distinct positive linear trend in the global warming component is linked to a drying of most of Northeast and Southeast Brazil. We propose that the linking mechanism between these SST and precipitation patterns is the intensification of the Hadley circulation (Hu and Fu, 2007) and, consequently, of the subsidence at the South Atlantic Subtropical High (Carvalho et al., 2011).

The same methodology is then applied to CMIP6 present-climate simulations (Table 1) to evaluate the capability of CMIP6 models to simulate these precipitation drivers, thus creating a process-based model selection and weighting approach to

underpin the future climate analysis. From a total of 30 models, we select 15 models that are capable of simulating at least two (Table 2) of the main regional precipitation drivers.

The mechanism discovery methodology is then applied to the near-future (2020-2050) climate simulations of the selected models. We find that an ENSO-like pattern, tied to a generalised warming of the tropical oceans, is linked to an increase of precipitation in South Brazil and a decrease in Northeast Brazil (Fig. 3 and 4), consistently with the present-climate indication of an intensification of the Hadley circulation. This mechanistic view of regional precipitation changes can underpin the development of storylines in future studies to support decision-making bodies in the water-energy-food nexus.

We go further to provide a quantitative view of regional precipitation changes based on the IPCC WG1 approach, contrasting the uncertainty of precipitation changes using 30 CMIP6 models versus using the 15 selected models. We show that the approach increased model agreement, particularly in South Brazil and SASH region. In the next 30 years (Fig. 6), a noticeable reduction in uncertainty across all seasons is evident mostly from June to November. This period is characterised by a clear drying pattern due to the strengthening of SASH, intensified within the subset of selected models, which leads to a suppression of precipitation in Northeast and Southeast Brazil, possibly delaying the rainy season in these regions.

Our methodology ~~employs an approach focused on understanding~~ of model selection and weighting considers the ~~underlying~~ precipitation drivers rather than simply comparing CMIP6 model precipitation with observations. By selecting and weighting models mechanistically, we achieve a reduction of the epistemic uncertainty of precipitation changes in Brazil in the CMIP6 ensemble. ~~This approach, as highlighted by Shepherd (2014), is a more appropriate way to address the uncertainties of regional precipitation changes and to support physically sound storylines regarding shifts in precipitation patterns.~~The method is based on the discovery of statistical relationships between SST patterns and precipitation through the PLS and the assumption that models with an accurate representation of these statistical relationships have a better representation of atmospheric processes leading to precipitation. Considering that the atmospheric flow is the medium connecting SST and precipitation and the statistical significance of the PLS loadings, we believe this assumption to be robust. However, as with any data-driven methodology, there could be instances where confounding factors may influence the results; this highlights the need of other mechanistic approaches capable of isolating rainfall mechanisms individually, such as atmospheric rivers, convergence zones, hurricanes and fronts (Catto et al., 2015; Franco-Diaz et al., 2019; Perez et al., 2024).

Acknowledgments

This research results from the R&D project developed by MeteoIA for Engie Brazil, funded by ANEEL under Project No. PD-00403-0054/2022.

References

Adler, R. el at.: The Global Precipitation Climatology Project (GPCP) Monthly Analysis (New Version 2.3) and a Review of 2017 Global Precipitation, Atmosphere, 9, 138, doi: http://dx.doi.org/10.3390/atmos9040138, 2018

Bazzanela, A.C. et al.: Performance of CMIP6 models over South America, Clim. Dyn., doi: https://doi.org/10.1007/s00382-023-06979-1, 2023.

Dias, C.G., Reboita, M.S. Assessment of CMIP6 Simulations over Tropical South America. Revista Brasileira de Geografia Física, 14(3), 1282-1295, doi: https://doi.org/10.26848/rbgf.v14.3.p1282-1295, 2021.

Durkee, J. D., and Mote, T. L.: A climatology of warm-season mesoscale convective complexes in subtropical South America, Int. J. Climatol., doi:10.1002/joc.1961, 2009

Firpo, M. A. F. et al: Assessment of CMIP6 models' performance in simulating present-day climate in Brazil, Frontiers in Climate, 4, doi: https://doi.org/10.3389/fclim.2022.948499, 2022.

Grise, K. M. and Davis, S. M.: Hadley cell expansion in CMIP6 models, Atmos. Chem. Phys., 20, 5249–5268, https://doi.org/10.5194/acp-20-5249-2020, 2020.

Gutiérrez, J. M., et al.: Atlas. In Climate Change 2021: The Physical Science Basis. Contribution of Working Group I to the Sixth Assessment Report of the Intergovernmental Panel on Climate Change [Masson-Delmotte, V., P. Zhai, A. Pirani, S.L. Connors, C. Péan, S. Berger, N. Caud, Y. Chen, L.Goldfarb, M.I. Gomis, M. Huang, K. Leitzell, E. Lonnoy, J.B.R. Matthews, T.K.Maycock, T. Waterfield, O. Yelekçi, R. Yu, and B. Zhou (eds.)]. Cambridge University Press. In Press. Interactive Atlas available from http://interactive-atlas.ipcc.ch/, 2021.

Hawkins, E., and Sutton, R. The potential to narrow uncertainty in projections of regional precipitation change, Clim Dyn, 37, 407–418, doi: https://doi.org/10.1007/s00382-010-0810-6, 2011.

Hersbach, H., and Dee D. ERA5 reanalysis is in production. ECMWF Newsletter 147:7, 2016.

Hirahara, S., M. Ishii, and Y. Fukuda: Centennial-Scale Sea Surface Temperature Analysis and Its Uncertainty. J. Climate, 27, 57–75, doi: https://doi.org/10.1175/JCLI-D-12-00837.1, 2014.

Themeßl, M. J., Gobiet, A., and Leuprecht, A.: Empirical-statistical downscaling and error correction of daily precipitation from regional climate models, Int J Climatol, 31, 1530–1544. doi: 10.1002/joc.2168, 2011.

Lu, J., Vecchi, G. A., and Reichler T. : Expansion of the Hadley cell under global warming, Geophys. Res. Lett., 34, L06805, doi:10.1029/2006GL028443, 2007.

Perez, G. M. P., et al.: Atmospheric convergence zones stemming from large-scale mixing, Weather Clim. Dynam., 2, 475–488, doi: https://doi.org/10.5194/wcd-2-475-2021, 2021.

Perez, G. M. P., et al: Using a Synoptic-Scale Mixing Diagnostic to Explain Global Precipitation Variability from Weekly to Interannual Time Scales. J. Climate, 35, 8225–8243, doi: https://doi.org/10.1175/JCLI-D-22-0110.1, 2022.

Shepherd, T. G.: Atmospheric circulation as a source of uncertainty in climate change projections. Nature Geosci 7, 703–708, doi: https://doi.org/10.1038/ngeo2253, 2014.

Shepherd, T. G.:Storyline approach to the construction of regional climate change information, Proc. R. Soc. A, 475: 20190013. doi: http://doi.org/10.1098/rspa.2019.0013, 2019.

Shepherd, T. G., et al.: Storylines: an alternative approach to representing uncertainty in physical aspects of climate change, Climatic Change, 151, 555–571, doi: https://doi.org/10.1007/s10584-018-2317-9, 2018.

Wegelin, J. A.: A Survey of Partial Least Squares (PLS) Methods, with Emphasis on the Two-Blok Case, Rel. téc. Seattle: University of Washington, 2000.